



# A $\beta$ -sheet structure interacting peptide for intracellular protein delivery into human pluripotent stem cells and their derivatives

Seong Loong Lo<sup>a</sup>, Shixiong Lua<sup>b</sup>, Jianxing Song<sup>b,c</sup>, Shu Wang<sup>a,c,\*</sup>

<sup>a</sup> Institute of Bioengineering and Nanotechnology, 31 Biopolis Way, The Nanos #04-01, 138669 Singapore, Singapore

<sup>b</sup> Department of Biochemistry, National University of Singapore, 14 Science Drive 4, S3 #04-05, 117543 Singapore, Singapore

<sup>c</sup> Department of Biological Sciences, National University of Singapore, 14 Science Drive 4, 117543 Singapore, Singapore

## ARTICLE INFO

### Article history:

Received 6 April 2012

Available online 19 April 2012

### Keywords:

Peptide

Protein delivery

Pluripotent stem cells

Self-assembly

## ABSTRACT

The advance in stem cell research relies largely on the efficiency and biocompatibility of technologies used to manipulate stem cells. In our previous study, we had designed an amphipathic peptide RV24 that can deliver proteins into cancer cell lines efficiently without significant side effects. Encouraged by this observation, we moved forward to test whether RV24 could be used to deliver proteins into human embryonic stem cells and human induced pluripotent stem cells. RV24 successfully mediated protein delivery into these pluripotent stem cells, as well as their derivatives including neural stem cells and dendritic cells. Based on NMR studies and particle surface charge measurements, we proposed that hydrophobic domain of RV24 interacts with  $\beta$ -sheet structures of the proteins, followed by formation of “peptide cage” to facilitate delivery across cellular membrane. These findings suggest the feasibility of using amphipathic peptide to deliver functional proteins intracellularly for stem cell research.

© 2012 Elsevier Inc. All rights reserved.

## 1. Introduction

The isolation of human embryonic stem cells [1] and the ability to generate induced pluripotent stem cells from somatic cells [2–4] have provided potentially invaluable tools for development of regenerative medicine, cancer therapy, disease modeling and drug screening [5–7]. To study the basic biology of stem cells and to direct their differentiation into specific cell types, different techniques, such as electroporation, transfections, and viral transduction, have been applied to introduce genetic material into stem cells. However, there are various limitations and disadvantages associated with these methods, including high rate of cell mortality due to high voltage pulses during electroporation [8,9], low efficiency of non-viral vector [10], random integration of viral transgene, and suppression of transgene expression due to promoter silencing [11]. Therefore, intracellular delivery of proteins might be an alternative approach to genetic manipulation.

Due to poor cellular permeability of proteins, a common approach for intracellular protein delivery is to modify proteins by fusing the proteins with a “cell penetrating peptide” (CPP) sequence with membrane penetration ability and deliver the covalently modified proteins [12]. Although some of the CPP-fused

proteins seem promising in penetrating into cells [13,14], modification of protein sequence may result in loss of protein biological functions due to possible interference to conformational folding and urea denaturation that is required to increase the accessibility of internally buried cell penetrating sequence [15,16]. Moreover, the proteins might be susceptible to protease degradation in extracellular environment. To overcome this, efforts have been made to develop protein delivery systems that can encapsulate proteins in a biodegradable and biocompatible particle. One good example of such system is a report using nano- and micro-particulate poly(lactide-co-glycolide) (PLGA) to deliver growth factors into embryoid bodies for controlled differentiation of stem cells into vascular lineage [17].

With increasing number of reports using synthetic peptides for intracellular protein delivery [18], synthetic peptide might also be useful in delivery of proteins into stem cells, especially due to its flexibility to incorporate different functional domains that can overcome extra- and intra-cellular barriers, or achieve cell type-specific delivery. Synthetic peptides can be produced, modified, purified and characterized without complicated instrumentations or chemistry. Most importantly, synthetic peptides are biodegradable to naturally occurring molecules, namely amino acids. Due to their low molecular weight, synthetic peptides are usually less immunogenic compared to lipids and polymers [19]. In our previous study, we had designed an amphipathic peptide RV24 that can deliver proteins into cancer cell lines efficiently without significant side effects [20]. Encouraged by this observation, we carried onto

\* Corresponding author at: Department of Biological Sciences, National University of Singapore, 14 Science Drive 4, 117543 Singapore, Singapore. Fax: +65 6779 2486.

E-mail addresses: [dbsws@nus.edu.sg](mailto:dbsws@nus.edu.sg), [swang@ibn.a-star.edu.sg](mailto:swang@ibn.a-star.edu.sg) (S. Wang).

evaluate its protein delivery efficiency in human pluripotent stem cells, including human embryonic stem cells and human induced pluripotent stem cells, as well as their derivatives, including neural stem cells and dendritic cells. We also investigated the possible self-assembly mechanism between RV24 and proteins using NMR.

## 2. Materials and methods

### 2.1. Peptide and proteins

The amphipathic peptide RV24 (sequence: RRRRRRRRRGPGVT WTPQAWFQWV) was prepared using a conventional solid-phase, chemical synthetic method (GL Biochem, Shanghai, China) and has the purity over 98%. The peptide stock solution was prepared by reconstituting lyophilized peptide in Milli-Q water (Millipore, Singapore) and was stored at  $-20^{\circ}\text{C}$  before usage. A 119 kDa sub-unit of  $\beta$ -galactosidase ( $\beta$ -gal) was purchased from Active Motif (Tokyo, Japan), enhanced green fluorescent protein (eGFP) was from Biovision (CA, USA), QuantiLum<sup>®</sup> recombinant firefly luciferase was from Promega (Singapore). Major sperm protein (MSP) and  $^{15}\text{N}$  isotope-labeled MSP ( $^{15}\text{N}$ -MSP) were expressed and purified as described in the previous publication [21]. To label MSP with fluorescein isothiocyanate (FITC, Product # F4274, Sigma Aldrich, Singapore), 50  $\mu\text{l}$  of FITC solution (1 mg/ml in 0.1 M sodium carbonate–bicarbonate buffer of pH 9.0) was mixed with 1 ml of MSP solution (2 mg/ml in  $1\times\text{PBS}$ ). The mixture was incubated for 8 h at room temperature with intermittent mixing, followed by dialysis in  $1\times\text{PBS}$  for 48 h using dialysis tubing with molecular weight cutoff of 1 kDa (Spectrum Laboratories, CA, USA). Absorbance readings at 280 and 495 nm of the FITC–MSP were taken after the dialysis to determine the Fluorescein/Protein (F/P) molar ratio. FITC-labeled protein A was from Invitrogen (Singapore). All the proteins were kept at  $-80^{\circ}\text{C}$  before usage.

### 2.2. Cell culturing

Human glioblastoma cell line U87 was grown in DMEM (Invitrogen, Singapore) supplemented with 10% fetal bovine serum (Thermo Scientific HyClone<sup>®</sup>, Singapore), 1% penicillin/streptomycin (Invitrogen, Singapore) and 1% L-glutamine (Invitrogen, Singapore). Human embryonic stem cell line H1 (H1 hES) was from WiCell (Madison, WI, USA). Induced pluripotent stem (iPS) cells were generated from human foreskin fibroblasts (Millipore, Bedford, MA) using Human STEMCCA Cre-Excisable Constitutive Polycistronic (OKSM) Lentivirus Reprogramming Kit (Millipore, Bedford, MA). H1 hES cells and iPS cells were cultured in feeder-free conditions in compliance with the protocol stated in the technical manual: 'Maintenance of hESCs in mTeSR™1' (StemCell Technologies, Vancouver, BC, Canada). H1 hES-derived dendritic cells (DCs) and iPS-derived neural stem cells (NSC) were generated and maintained as previously reported [22,23]. All the cells were maintained in a humidified incubator with 5%  $\text{CO}_2$  at  $37^{\circ}\text{C}$ .

### 2.3. Delivery and detection of $\beta$ -galactosidase

Human pluripotent stem cells (H1 hES and iPS) were seeded in cell culture well-plate one day before  $\beta$ -gal delivery. To prepare RV24/ $\beta$ -gal complex,  $\beta$ -gal was mixed with RV24 in  $1\times\text{PBS}$  at molar ratio of 100. After incubation for 30 min at room temperature, the complex was incubated with cells in serum-free medium for 4 h, followed by cell culture medium for 20 h. To detect  $\beta$ -gal using  $\beta$ -gal staining kit (Active Motif, Tokyo, Japan), cells were washed with  $1\times\text{PBS}$ , fixed with fixing solution for 5 min, washed twice with  $1\times\text{PBS}$ , and stained with staining solution for 2 h. Staining

solution was replaced with  $1\times\text{PBS}$  and bright field images were taken by inverted microscope (Olympus, Singapore).

### 2.4. Delivery of eGFP and flow cytometric analysis

NSCs were seeded in cell culture well-plate 1 day before eGFP delivery. DCs were prepared in suspension immediately before eGFP delivery. The RV24/eGFP complex was prepared and incubated with the cells as described in previous section. Flow cytometric analysis was done 4 h after complex incubation with cells. The medium that might contain floating cells was first collected in 5 ml round bottom test tube. The cells were washed with  $1\times\text{PBS}$  and trypsinized with  $1\times\text{EDTA}$ –trypsin for 5–10 min at  $37^{\circ}\text{C}$ . After confirming cell detachment under inverted microscope, the cells were then resuspended in cell culture medium and transferred to the 5 ml round bottom test tube containing the collected medium. The cells were centrifuged at 1000 rpm for 5 min, washed with  $1\times\text{PBS}$ , resuspended in  $1\times\text{PBS}$  and analyzed with a FACSCalibur flow cytometer (BDIS, Singapore) by counting 10,000 events.

### 2.5. Determination of CMC of RV24 and surface charge of RV24/protein complex

The critical micelle concentrations (CMC) of RV24 and sodium dodecyl sulfate (SDS) were determined in water using a multichannel microtensiometer (Kibron Delta-8; Kibron, Espoo, Finland). Serial dilution of tested materials was done in 96-well plate. The tested materials were transferred to DynePlate (Kibron, Espoo, Finland) and incubated for 10 min at room temperature to achieve sufficient equilibration before measurement. For zeta potential measurement, all the samples were prepared at a protein concentration of 20  $\mu\text{g}$  in 750  $\mu\text{l}$  Milli-Q water. Zeta potentials were measured electrophoretically using Zetasizer Nano-ZS (Malvern Instruments, Malvern, UK) at room temperature. The zeta potential plot was generated by superimposing multiple spectra for each sample and the zeta potential is presented as mean with SD ( $n = 4$ ).

### 2.6. Delivery of FITC–MSP and NMR studies of RV24/ $^{15}\text{N}$ -MSP complex

Delivery of FITC–MSP was carried out with U87 cells seeded on 96-well plate, as described previously. After incubation for 4 h, bright field and fluorescent images were taken separately by fluorescent inverted microscope (Olympus, Singapore) and superimposed with Adobe Photoshop (Adobe Systems Incorporated, CA, USA). For nuclear magnetic resonance (NMR) studies, both  $^{15}\text{N}$ -MSP protein and RV24 were prepared in  $1\times\text{PBS}$ . Two-dimensional  $^1\text{H}$ – $^{15}\text{N}$  heteronuclear single quantum coherence (2D-HSQC) NMR experiments were conducted at fixed MSP concentration of 200  $\mu\text{M}$  and subsequently titrated with increasing concentration of RV24. All NMR data were collected at  $25^{\circ}\text{C}$  on an 800 MHz Bruker Avance spectrometer (Bruker, Singapore) equipped with a shielded cryoprobe. All spectra were processed and viewed using the CCPNMR software [24]. By superimposing the HSQC spectra, the shifted HSQC peaks were identified and further assigned to the corresponding residues of the MSP domain whose assignment was previously achieved [21].

## 3. Results and discussion

### 3.1. Delivery of proteins into human pluripotent stem cells and their derivatives

Encouraged by the efficiency and biocompatibility of RV24 in different cancer cell lines [20], we assessed the capability of RV24 to deliver protein into two types of human pluripotent stem

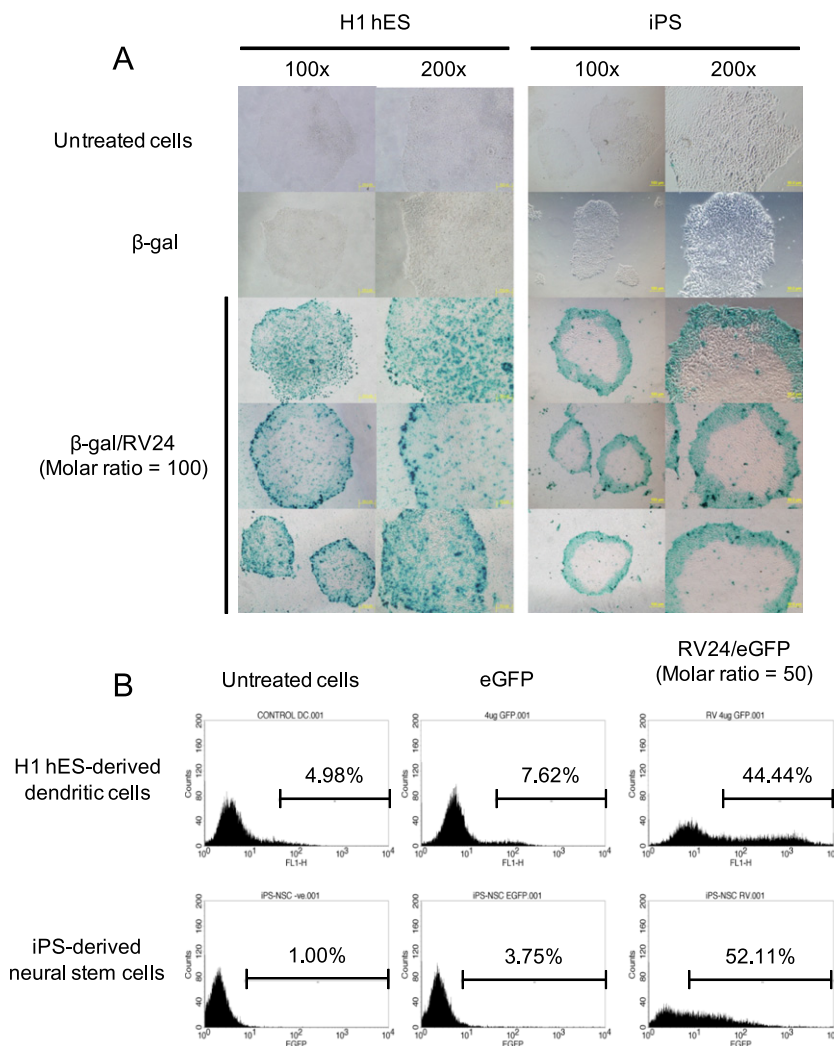


**Fig. 1.** RV24 successfully delivers proteins into human pluripotent stem cells and their derivatives. (A) Human embryonic stem cell line H1 (H1 hES) and induced pluripotent stem cells (iPS) were treated with RV24/β-gal complex prepared at molar ratio of 100 for 24 h before staining. Images of different positively stained colonies were taken at magnification of 100× and 200×. (B) H1 hES-derived dendritic cells and iPS-derived neural stem cells were treated with RV24/eGFP complex prepared at molar ratio of 50 for 4 h before flow cytometric analysis. The value in percentage is the percentage of eGFP<sup>+</sup> cells detected in a population count of 10,000 events.

cells, human embryonic stem cell line H1 (H1 hES) and induced pluripotent stem cells (iPS) generated from human foreskin fibroblasts. Beta-gal staining showed very promising results, with positively-stained cells located not only at the periphery ring region of the colonies that has usually differentiated cells, but also at the inner region of the colonies that contains the pluripotent stem cells (Fig. 1A). This result demonstrates the potential of RV24 in stem cell research, such as directed differentiation by delivery of growth factors [17]. RV24 also successfully delivered eGFP into H1 hES-derived dendritic cells (DC) and iPS-derived neural stem cells (NSC), with up to 44% of eGFP<sup>+</sup> DCs and 52% of eGFP<sup>+</sup> NSC detected in flow cytometric analysis (Fig. 1B). This could be useful in presentation of cancer-related antigen for DC-based cancer immunotherapy [25–27], and loading of protein-based therapeutics for NSC-based metastatic cancer therapy.

### 3.2. Mechanism of RV24/protein complex formation

Although RV24 successfully delivers cargo proteins into pluripotent stem cells and their derivatives, we would like to identify the functional proteins that can be delivered, by gaining insight into mechanism of RV24/protein complex formation. We first investigated whether RV24 forms a peptide micelle due to its

amphipathicity before complex formation [28]. We measured the critical micelle concentration (CMC) of RV24 by serially diluting 5 mg/ml peptide solution that was approximately 20-fold more concentrated than the peptide solution used in preparation of RV24/protein complex. Compared to the standard, sodium dodecyl sulfate (SDS), with CMC value of 2.5 mg/ml, RV24 did not form any micelle within the tested concentration range (Fig. 2A). Therefore, the RV24/protein complex formation is not due to the interaction between peptide micelles and proteins, but through direct interactions between proteins and peptides.

Two types of direct interactions might be involved in complex formation: (1) hydrophobic interaction between β-sheet on surface of proteins and tryptophan-rich hydrophobic domain of RV24, and (2) electrostatic interaction between negatively charged site on surface of proteins and arginine-rich hydrophilic domain of RV24. To identify the type of interaction and the corresponding interaction site on the protein, we employed the two-dimensional <sup>1</sup>H–<sup>15</sup>N heteronuclear single quantum coherence nuclear magnetic resonance (2D-HSQC NMR) techniques by monitoring peak shifts in the 2D-HSQC NMR spectra of the free protein and in the presence of RV24. In this study, recombinant major sperm protein domain (MSP) of human vesicle-associated membrane protein-associated protein B was chosen since the structure of MSP had already been

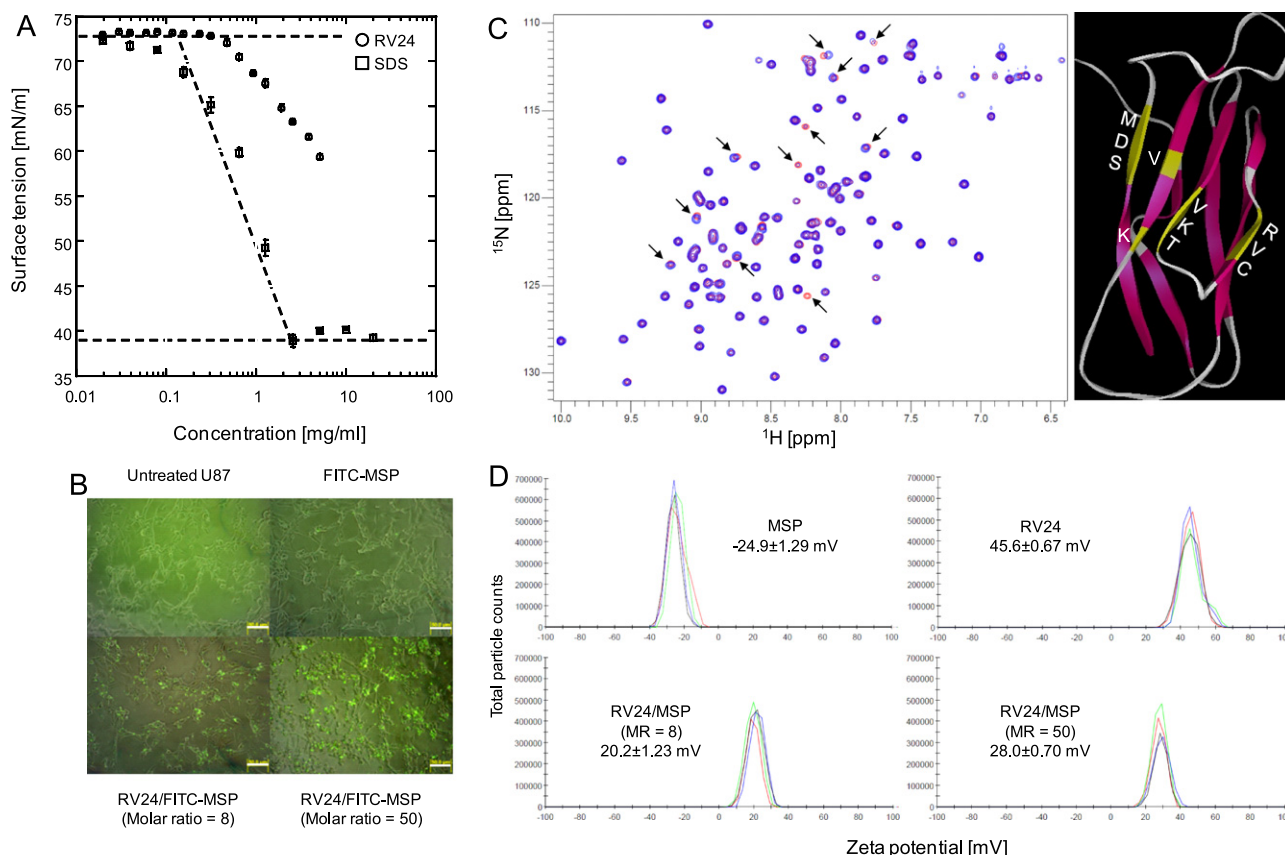


**Fig. 2.** Mechanism of RV24/protein complex formation. (A) Critical micelle concentration of RV24 was determined based on a plot of water surface tension vs. concentration of sample measured at room temp using multichannel microtensiometer. Sodium dodecyl sulfate (SDS) was included as a standard. (B) Delivery of FITC-MSP protein into U87 cells with RV24. The images were superimposition of bright field and fluorescent images taken 4 h after protein delivery. Scale bar = 50 μm. (C) (Left panel) Superimposition of 2D <sup>1</sup>H-<sup>15</sup>N heteronuclear single quantum coherence (HSQC) NMR spectra of MSP protein in the free state (blue) and in the presence of RV24 (red). Peak shifts were marked with arrows. (Right panel) Residues corresponding to peak shifts mapped onto 3D structure of MSP protein (PDB-3IKK). The ribbons in red are β-strands and the affected residues are marked in yellow. (D) Zeta potentials of MSP, RV24 and RV24/MSP complex (molar ratio of 8 and 50) were measured electrophoretically at room temp. The zeta potential is presented as mean with SD ( $n = 4$ ) (For interpretation of the references to color in this figure legend, the reader is referred to the web version of this article).

determined by X-ray crystallography and extensively characterized by NMR spectroscopy in previous study [21], and RV24 is capable of delivering FITC-labeled MSP (FITC-MSP) into U87 cells at a molar ratio of 50 (Fig. 2B). When RV24 was gradually titrated into <sup>15</sup>N-MSP protein, peak shifting was observed on the 2D-HSQC NMR spectra and saturated at a molar ratio of 8 (Fig. 2C left panel). By comparing to previously assigned 2D-HSQC NMR spectrum [21], 11 residues corresponding to the perturbed peaks were assigned, including Val44, Lys45, Thr46, Cys53, Val54, Arg55, Lys87, Val90, Met115, Asp116, and Ser117. Three of the residues are positively charged and one of them is negatively charged, while the rest are uncharged. Since RV24 does not contain any negatively charged amino acid residues, it is highly unlikely that the electrostatic interaction significantly contributes to the binding affinity. Mapping the perturbed 11 amino acid residues onto the 3D structure of MSP (PDB ID: 3IKK) reveals that 10 out of 11 amino acid residues are located within the β-sheet structure spanning across four β-strands (Fig. 2C right panel). Although Lys87 is not on the β-sheet structure, it is located right beside one of the β-strands. These findings suggest that binding of RV24 occurs on β-sheet structure on the surface of MSP mainly through hydrophobic interaction. This hypothesis is also consistent with the observation on 3D structures of β-gal (PDB ID: 3I3E) and eGFP (PDB ID: 3A14), showing easily accessible β-sheet structures on the surface of the proteins.

Since β-gal, eGFP, and MSP are negatively charged proteins with β-sheet structures (Table 1), we tried to use RV24 to deliver two other proteins that have mainly α-helices on protein surface, positively charged recombinant firefly luciferase (PDB ID: 1LCI) and

negatively charged FITC-labeled Protein A (PDB ID: 2JWD). However, we could not detect bioluminescence from cell lysate and fluorescence inside the tested cell lines after delivery of the above proteins. These results suggest that accessible β-sheet structures on protein surface are essential interaction sites for binding of RV24. Unlike complex formation of DNA and peptide-based carriers through electrostatic interaction [29], the surface charge of the cargoes, proteins in this case, is not a crucial factor. To the best of our knowledge, our study on the mechanism of peptide/protein complex formation is the first demonstration of using 2D-HSQC NMR for identification of interaction site essential for interaction between peptide carrier and protein cargo.

One interesting finding from 2D-HSQC NMR experiments is that the peak shifting was saturated at molar ratio of 8 but this molar ratio is not efficient for protein delivery when compared to molar ratio of 50 (Fig. 2B). Previous publications proposed that amphipathic peptide Chariot™ forms complex with protein through hydrophobic interaction followed by a “peptide cage” formation for intracellular delivery [30–32]. Therefore, it is possible that some molecules of RV24 will first bind to hydrophobic domain on surface of proteins, following the formation of “peptide cage” surrounding the RV24/protein complex. An indirect way to verify this is by measuring zeta potential of free MSP, free RV24, and RV24/MSP complex formed at molar ratios of 8 and 50. The zeta potential measurements showed that MSP was negatively charged and RV24 was highly positively charged (Fig. 2D). RV24/MSP complex prepared at molar ratio of 8 had distinct peaks centered at zeta potential of +20 mV. Based on the 2D-HSQC NMR findings,



**Table 1**

List of proteins used in the current study.

Protein	PDB ID	2° Structure on protein surface	Molecular wt. (kDa)	Zeta potential (mV)	Deliverable by RV24
β-Gal subunit	3I3E	β-Sheet	119	−51.9	Yes
eGFP	3A14	β-Sheet	29	−31.8	Yes
MSP	3IKK	β-Sheet	16	−24.9	Yes
Luciferase	1LCI	α-Helix	61	+8.2	No
Protein A	2JWD	α-Helix	42	−28.6	No

the positive charge of the complex was probably not due to electrostatic interaction, but due to the binding of RV24 to β-sheet of MSP that resulted in change of overall surface charge of MSP. When the RV24/MSP complexes were prepared at molar ratio of 50, the zeta potential of the complex increased to +28 mV. The presence of distinct peaks and the increase in zeta potential indirectly proves that molecules of RV24 that could not bind to hydrophobic domain of MSP, instead of staying freely in solution, continue to “aggregate” on the surface of the pre-formed RV24/MSP complexes. Since the electrostatic interaction between protein and RV24 is assumed to have minimal contribution to complex formation based on 2D-HSQC NMR findings and unavailable delivery of negatively charged FITC-labeled Protein A, it is highly possible that the positively charged CPP sequence will face out of the complex to facilitate delivery across cellular membrane, instead of interacting with negatively-charged amino acids of protein.

Understanding that the main interaction site on the protein is β-sheet structure, we can easily identify the proteins that can be delivered by RV24 peptide if the 3D structures of the proteins are well-characterized. To the best of our knowledge, this is the first study to demonstrate the possibility of using peptide for intracellular protein delivery into human pluripotent stem cells and to identify the interaction site for peptide/protein complex formation using 2D-HSQC NMR. This simple yet efficient peptide/protein self-assembly technology should have great potentials for intracellular delivery of functional proteins into pluripotent stem cells for stem cells biology research and their derivatives for therapeutic applications.

## Acknowledgments

This work was supported by Institute of Bioengineering and Nanotechnology (Biomedical Research Council, Agency for Science, Technology and Research, Singapore) and Grants from National Medical Research Council in Singapore (NMRC/1203/2009 & NMRC/IRG10Nov122), Ministry of Education of Singapore (MOE2011-T2-1-056), and Agency for Science, Technology and Research, Singapore (JCO 11/03/FG/07/02) awarded to S. Wang.

## References

- [1] J.A. Thomson, J. Itskovitz-Eldor, S.S. Shapiro, M.A. Waknitz, J.J. Swiergiel, V.S. Marshall, J.M. Jones, Embryonic stem cell lines derived from human blastocysts, *Science* 282 (1998) 1145–1147.
- [2] I.H. Park, R. Zhao, J.A. West, A. Yabuuchi, H. Huo, T.A. Ince, P.H. Lerou, M.W. Lensch, G.Q. Daley, Reprogramming of human somatic cells to pluripotency with defined factors, *Nature* 451 (2008) 141–146.
- [3] K. Takahashi, K. Tanabe, M. Ohnuki, M. Narita, T. Ichisaka, K. Tomoda, S. Yamanaka, Induction of pluripotent stem cells from adult human fibroblasts by defined factors, *Cell* 131 (2007) 861–872.
- [4] J. Yu, M.A. Vodyanik, K. Smuga-Otto, J. Antosiewicz-Bourget, J.L. Frane, S. Tian, J. Nie, G.A. Jonsdottir, V. Ruotti, R. Stewart, Slukvin II, J.A. Thomson, Induced pluripotent stem cell lines derived from human somatic cells, *Science* 318 (2007) 1917–1920.
- [5] S.M. Wu, K. Hochedlinger, Harnessing the potential of induced pluripotent stem cells for regenerative medicine, *Nat. Cell Biol.* 13 (2011) 497–505.
- [6] S.M. Hussein, K. Nagy, A. Nagy, Human induced pluripotent stem cells: the past, present, and future, *Clin. Pharmacol. Ther.* 89 (2011) 741–745.
- [7] M. Grskovic, A. Javaherian, B. Strulovici, G.Q. Daley, Induced pluripotent stem cells – opportunities for disease modelling and drug discovery, *Nat. Rev. Drug Discov.* 10 (2011) 915–929.
- [8] W.J. Buchser, J.R. Pardinas, Y. Shi, J.L. Bixby, V.P. Lemmon, 96-well electroporation method for transfection of mammalian central neurons, *Biotechniques* 41 (2006) 619–624.
- [9] P.D. Peng, C.J. Cohen, S. Yang, C. Hsu, S. Jones, Y. Zhao, Z. Zheng, S.A. Rosenberg, R.A. Morgan, Efficient nonviral sleeping beauty transposon-based TCR gene transfer to peripheral blood lymphocytes confers antigen-specific antitumor reactivity, *Gene Ther.* 16 (2009) 1042–1049.
- [10] L. Ferreira, Nanoparticles as tools to study and control stem cells, *J. Cell. Biochem.* 108 (2009) 746–752.
- [11] X. Xia, Y. Zhang, C.R. Zieth, S.C. Zhang, Transgenes delivered by lentiviral vector are suppressed in human embryonic stem cells in a promoter-dependent manner, *Stem Cells Dev.* 16 (2007) 167–176.
- [12] M. Mae, U. Langel, Cell-penetrating peptides as vectors for peptide, protein and oligonucleotide delivery, *Curr. Opin. Pharmacol.* 6 (2006) 509–514.
- [13] S. Asoh, S. Ohta, PTD-mediated delivery of anti-cell death proteins/peptides and therapeutic enzymes, *Adv. Drug Deliv. Rev.* 60 (2008) 499–516.
- [14] J.S. Wadia, S.F. Dowdy, Transmembrane delivery of protein and peptide drugs by TAT-mediated transduction in the treatment of cancer, *Adv. Drug Deliv. Rev.* 57 (2005) 579–596.
- [15] B.J. Bennion, V. Daggett, The molecular basis for the chemical denaturation of proteins by urea, *Proc. Natl. Acad. Sci. USA* 100 (2003) 5142–5147.
- [16] G.B. Rainer Rudolph, Hauke Lilie, Rainer Jaenicke, *Folding Proteins*, second ed., Oxford University Press, New York, 1997.
- [17] B.J. Conley, A.O. Trounson, R. Mollard, Human embryonic stem cells form embryoid bodies containing visceral endoderm-like derivatives, *Fetal Diagn. Ther.* 19 (2004) 218–223.
- [18] S.L. Lo, S. Wang, Intracellular protein delivery systems formed by noncovalent bonding interactions between amphipathic peptide carriers and protein cargos, *Macromol. Rapid Commun.* 31 (2010) 1134–1141.
- [19] J.W. Fabre, L. Collins, Synthetic peptides as non-viral DNA vectors, *Curr. Gene Ther.* 6 (2006) 459–480.
- [20] S.L. Lo, S. Wang, Evaluation of the use of amphipathic peptide-based protein carrier for in vitro cancer research, *Biochem. Biophys. Res. Commun.* 419 (2012) 170–174.
- [21] J. Shi, S. Lua, J.S. Tong, J. Song, Elimination of the native structure and solubility of the hVAPB MSP domain by the Pro56Ser mutation that causes amyotrophic lateral sclerosis, *Biochemistry* 49 (2010) 3887–3897.
- [22] M.A. Slukvin II, J.A. Vodyanik, M.E. Thomson, K.D. Choi, Gumenyuk, Directed differentiation of human embryonic stem cells into functional dendritic cells through the myeloid pathway, *J. Immunol.* 176 (2006) 2924–2932.
- [23] J. Yang, D.H. Lam, S.S. Goh, E.X. Lee, Y. Zhao, F.C. Tay, C. Chen, S. Du, G. Balasundaram, M. Shahbazi, C.K. Tham, W.H. Ng, H.C. Toh, S. Wang, Tumor tropism of intravenously injected human induced pluripotent stem cell-derived neural stem cells and their gene therapy application in a metastatic breast cancer model, *Stem Cells* (2012).
- [24] W.F. Vranken, W. Boucher, T.J. Stevens, R.H. Fogh, A. Pajon, M. Llinas, E.L. Ulrich, J.L. Markley, J. Ionides, E.D. Laue, The CCPN data model for NMR spectroscopy: development of a software pipeline, *Proteins* 59 (2005) 687–696.
- [25] T. Akagi, X. Wang, T. Uto, M. Baba, M. Akashi, Protein direct delivery to dendritic cells using nanoparticles based on amphiphilic poly(amino acid) derivatives, *Biomaterials* 28 (2007) 3427–3436.
- [26] K. Palucka, H. Ueno, J. Fay, J. Banchereau, Dendritic cells and immunity against cancer, *J. Intern. Med.* 269 (2011) 64–73.
- [27] E.M. Stier, M. Mandal, K.D. Lee, Differential cytosolic delivery and presentation of antigen by listeriolysin O-liposomes to macrophages and dendritic cells, *Mol. Pharm.* 2 (2005) 74–82.
- [28] D.W. Ryu, H.A. Kim, H. Song, S. Kim, M. Lee, Amphiphilic peptides with arginines and valines for the delivery of plasmid DNA, *J. Cell. Biochem.* 112 (2011) 1458–1466.
- [29] P. Saccardo, A. Villaverde, N. Gonzalez-Montalban, Peptide-mediated DNA condensation for non-viral gene therapy, *Biotechnol. Adv.* 27 (2009) 432–438.
- [30] S. Deshayes, A. Heitz, M.C. Morris, P. Charnet, G. Divita, F. Heitz, Insight into the mechanism of internalization of the cell-penetrating carrier peptide Pep-1 through conformational analysis, *Biochemistry* 43 (2004) 1449–1457.
- [31] S. Deshayes, M.C. Morris, G. Divita, F. Heitz, Interactions of amphipathic carrier peptides with membrane components in relation with their ability to deliver therapeutics, *J. Pept. Sci.* 12 (2006) 758–765.
- [32] S. Deshayes, T. Plenat, P. Charnet, G. Divita, G. Molle, F. Heitz, Formation of transmembrane ionic channels of primary amphipathic cell-penetrating peptides. Consequences on the mechanism of cell penetration, *Biochim. Biophys. Acta* 1758 (2006) 1846–1851.